

## Design of novel tilting electric four-wheelers

### Design eines neuartigen neigbaren elektrischen 4-Rad-Fahrzeugs

Francesco Bucchi, Francesco Frendo

Department of Civil and Industrial Engineering, Università di Pisa, Pisa, Italy

Dragan Simic

AIT Austrian Institute of Technology GmbH, Wien, Austria

Onorino di Tanna

Piaggio & C. Spa, Pontedera, Italy

Martin Perterer

KTM Technologies GmbH, Salzburg/Anif, Austria



*This project has received funding from the European Union's Horizon 2020 research and innovation programme under grant agreement nr 653511*



**EGVI**  
European Green  
Vehicles Initiative

RESOLVE



RANGE OF ELECTRIC SOLUTIONS FOR L CATEGORY VEHICLES

## Abstract

EU cities are increasingly congested due to the demand and usage of motor vehicles. Future scenarios for EU urban centers see a modal shift in personal mobility from cars to lighter, smaller, more specialized and environmental-friendly alternatives.

Electric L-category Vehicles (ELVs) are viable alternatives that can fulfill the commuter needs due to their small size and light-weight: by consequence the energy requirement, battery size and related costs can be strongly reduced respect to conventional electric cars.

However, this modal shift must overcome one main challenge: most car drivers do not consider L-category vehicles as a suitable option mainly due to L-vehicle dynamic limitations. To achieve that, the RESOLVE (Range of Electric SOLUTIONS for L-category VEHICLES) project, funded in the Horizon 2020 framework - Green Vehicles GV5-2014 call, will develop components and systems aimed to meet the low cost target required for this segment. At the same time, the project will deliver an exciting and attractive ELV driving experience by proposing new concepts (tilting and narrow track), while containing as much as possible the vehicle energy consumption.

In this paper, the dynamics analyses carried out to develop the architecture of ELV vehicles are presented. A stability analysis of the vehicles in straight line was firstly carried out and the results were compared to tilting two and three-wheelers for a wide range of speed. A detailed multibody model was developed to simulate the steady-state behavior of the 4-wheelers during turning and to perform further dynamic analyses. In addition, an entire vehicle model including electrical and mechanical components (battery, power electronics, e-motor, driveline, etc.) was developed to assess the ELVs energy needs during reference and real-world driving maneuver.

The results demonstrated the feasibility of this novel kind of vehicles, confirming the exciting driving experience typical of tilting vehicles, combined with comfort, low environmental impact and limited energy requirements.

## **Design of novel tilting electric four-wheelers**

# 1 Introduction

Although ELV can fulfill most of the commuter needs due to their small size, light weight, low on board energy requirement and thus smaller batteries, their market share is still not relevant and, beside the low consumption achievable, have often limited handling capabilities. Within this project the driving experience is taken in the utmost regards by implementing a novel vehicle architecture aimed to ensure an effective and enjoyable riding dynamics similar to the motorcycle one while maintaining limited small transversal dimension.

This target can be achieved by implementing tilting multi-wheels architectures able to achieve a completely free roll motion, so that the wheels of each axle have the same roll angle of the vehicle frame maintaining all the external forces aligned with the vehicle vertical symmetry plane (Fig. 1): in this way no vertical load transfer is requested from left to right side.

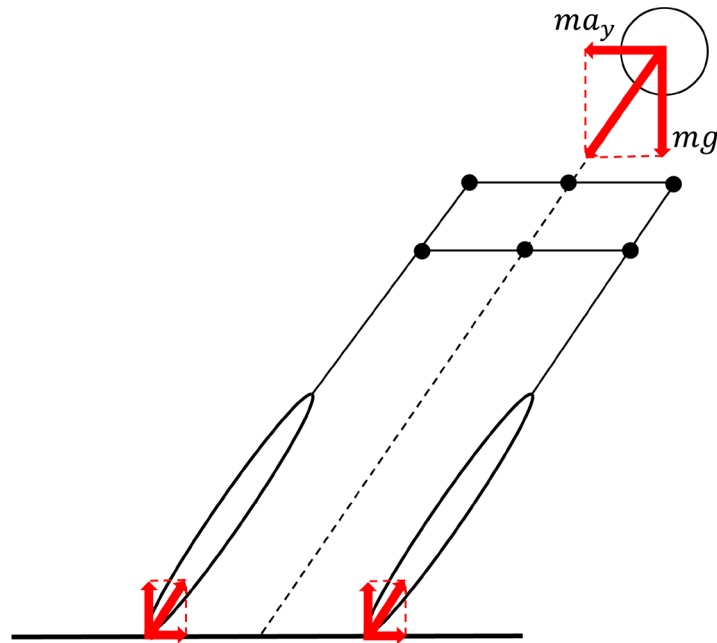


Figure 1. Roll equilibrium of tilting multi wheel vehicle

The equal split between the two wheels in all cornering conditions guarantees the optimal usage of tire performances. Indeed, due to the strong non-linear behavior of road-tire adherence depending on vertical load, the wheels can reach greater lateral acceleration values giving more safety margin in evasive maneuvers with respect to both conventional two wheelers and ELVs.

A similar architecture has been successfully exploited on the market thanks to vehicles with two front wheels like the Piaggio MP3. In the RESOLVE project, the concept will be further stressed by apply-

ing similar architectures to narrow four wheelers powered by electric powertrains in order to extend the obvious advantages also to the rear axle in order to increase static and dynamic stability and to allow for the investigation of advanced vehicle control functions (eg. torque vectoring). Two slightly different concepts for 4-wheeler tilting vehicles are considered that can be categorized in the L2e and L6e vehicle class. Both vehicles are designed for two people and a certain amount of luggage space.

## **2 Tilting four-wheeler vehicle description**

The L2e vehicle consists of an aluminium alloy main structure that connects the front and the rear tilting components. The front suspension and tilting mechanism is based on a pseudo-McPherson concept. The rear suspension and tilting mechanism includes two separate swing arms with integrated motors and gear reduction with pull type spring-dampers. A torque vectoring principle allows for flexible power distribution between the two rear wheels and therefore enables the potential for investigation of innovative driving assistance functions for vehicle active safety improvement.

The L6e vehicle consists of a metallic mainframe partly made of aluminium alloy extrusion profiles, steel pipes and a structural battery case. This main structure is combined with a steel tubes roll cage covered with panels for weather protection and with two tilting substructures on front and back axles. The front suspension and tilting mechanism is based on a double transversal wishbone concept. The rear suspension and tilting mechanism consists of two swing arms with damper linked to a central rear tilting bar. The traction is provided to both rear wheels by a single electric motor encapsulated in the mainframe with a differential gear reduction with final belt transmission.

## **3 Longitudinal dynamics**

For the longitudinal modelling and simulation of the vehicle demonstrators the Modelica simulation language using Dymola simulation software was chosen. In this paper, for the sake of conciseness, the architecture considered for the simulation is the L6e one, even if an identical analysis was performed for the L6e vehicle.

The demonstrator containing all the electrical and mechanical components of the vehicle is shown in Fig. 2. The electrical components include the traction 48V battery, the electric motors, the inverters and all the auxiliary modules powered by a service 12 V battery (recharged through a DC/DC converter). To simplify the entire vehicle simulation the sum of the power auxiliaries (e.g. the vehicle control, the lights, the energy needed for 12 V system, etc.) are represented by auxiliaries module. The e-machine model is coupled through the transmission to the rear axle/tires. The inverter model is

schematically represented, but in the entire simulation model is the inverter model integrated into the e-machine model. The total gear ratio of the transmission from the electric motor to the wheels is a sensitive design variable and was therefore modified during the simulation process in the range from 8:1 to 28:1, verifying both acceleration and energy consumption targets on various driving conditions and reference cycles.

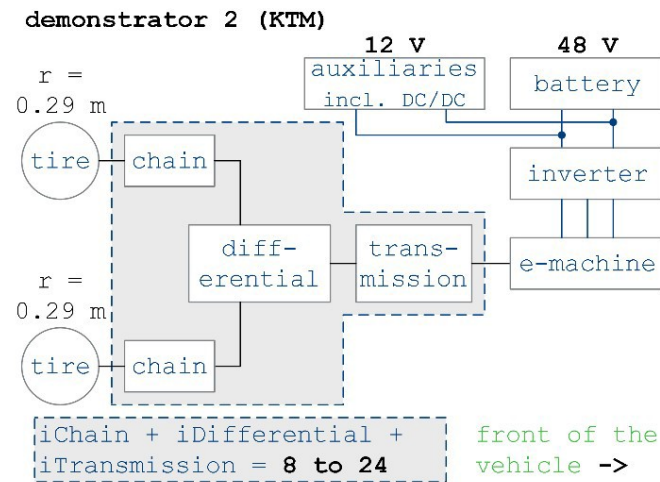


Figure 2. Electrical and mechanical architecture of the demonstrator 1 (KTM)

A simulation model for investigation and analysis of the demonstrator is shown in Fig. 3. The electrical four-wheel vehicle was modelled using the libraries SmartCooling [1] and SmartPowerTrains [2]. The powertrain models includes a battery (Bat.), an electrical machine (MG), a transmission including chain (Trans.) and a rear drive model (Axle Rear) including non-linear tires. A quasi-steady state model of the electrical machine with integrated converter and control system is used in the simulations and an idealized parametric battery model (Bat.) is used to supply the electrical machine and all the electrical components of the vehicle including auxiliaries (Aux.).

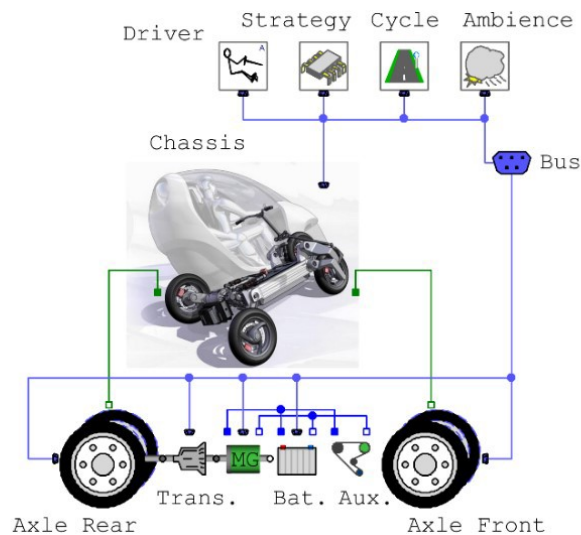


Figure 3. The Dymola using Modelica simulation model of the tilting four-wheeler

Both battery and electric motor/inverter are modeled on characteristic curves (operating maps) which can be easily calibrated based on measurement data or data sheets of the component manufacturer.

The battery model consists of a constant capacitor and a constant internal resistor with a state of charge (SOC) estimator designed as follows:

- if one cell is in the maximum state of charge (SOCMax) the output voltage of this cell is the maximum cell voltage (VCellMax);
- if the cell is discharged to the minimum state of charge (SOCMin) the output voltage of this cell is the minimum cell voltage (VCellMin).

As a consequence, the instantaneous output voltage level of the battery is associated with an instantaneous SOC. Figure 4 illustrates the relation between these two quantities used for the first simulation run.

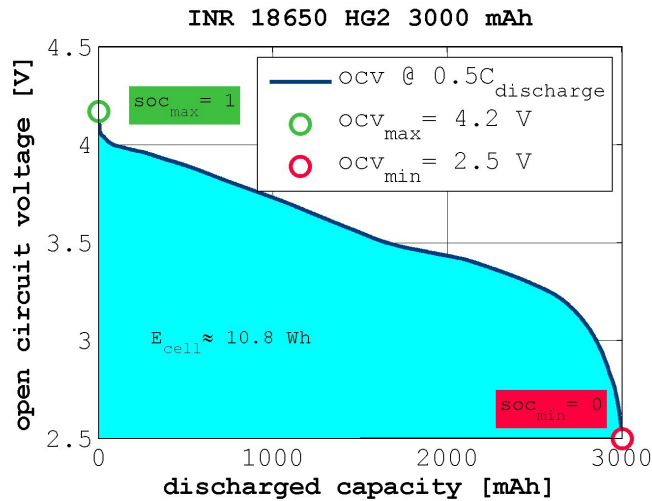


Figure 4. Relation between open source voltage and discharged capacity of the used cell at 3A discharge current

In order to effectively assess the vehicle performances depending on different driving styles and conditions, the following cycles have been considered: a) New European Driving Cycle (NEDC), b) Artemis, c) Worldwide Motorcycle Test Cycle (WMTC) and d) full load. Since the maximum vehicle speed is 45 km/h, the parts of the driving cycles which overcomes this speed values has been reduced to the maximum allowed speed of the demonstrators, as represented in Fig. 5 for WMTC.

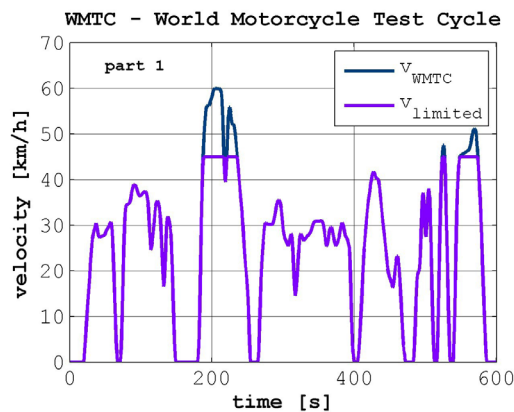


Figure 5. Part 1 of the Worldwide Motorcycle Test Cycle (WMTC), limited velocity

The same driving scenarios are simulated under all driving cycles by analyzing the sensitivity of energy consumption depending on both mass and gear ratio variations.

More than 300 simulation scenarios have been considered and analysed to identify the best gear ratio considering both energy consumption and acceleration performances of the vehicle. The analysis



shows that the best gear ratio of the transmission is in the range between 12 and 13. In Fig. 6a and Fig. 6b the analysed and described simulation results for the road-slopes 5% and 10% are depicted.

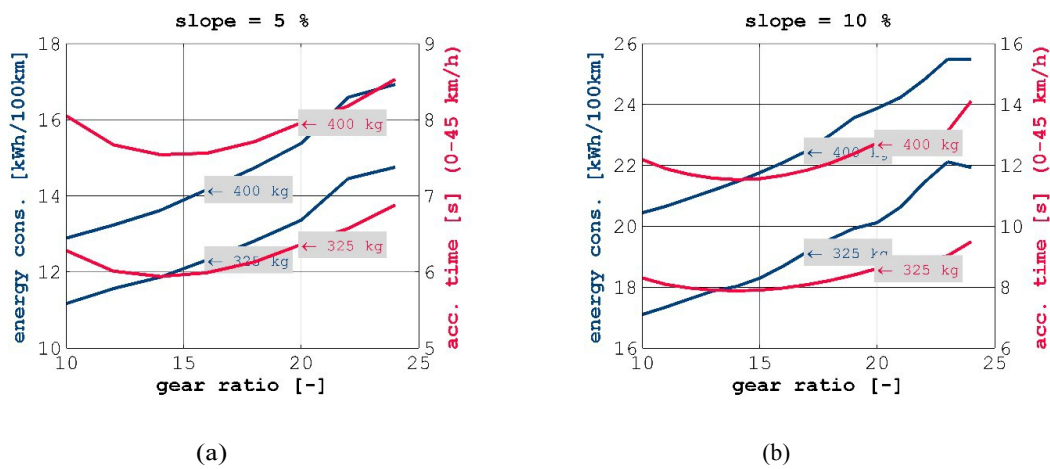


Figure 6. Acceleration performances and energy consumption for road-slope 5% (a) and 10% (b).

## 4 Lateral dynamics

In order to simulate the dynamic behaviour of the vehicle two different approaches were used:

- a numerical stability analysis of the tilting four-wheelers running in straight line at constant speed performed through a simplified model aimed at computing the vehicle eigen-modes;
- a multibody analysis including steady state and transient maneuvers (e.g. steering pad, double lane change, slalom etc.) performed using a specifically developed virtual rider.

### 4.1 Stability analysis of the rigid vehicle

The model developed for the stability analysis is shown in Fig. 11. It is composed of 23 rigid bodies, the suspension are assumed as infinitely rigid elements as well as the tire are modelled as rigid lenticular rings. The rider, which is not represented, is rigidly fixed to the main frame and the global center of gravity of the vehicle is assumed to be invariant in a vehicle reference frame.

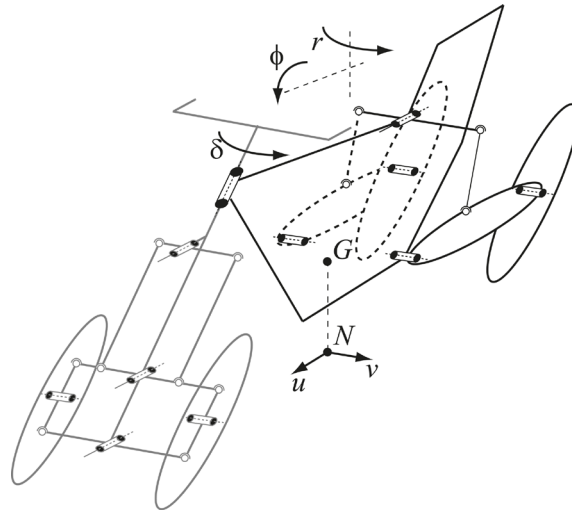


Figure 7. Stability analysis model and state variables.

Since the vehicle is equipped with front and rear tilting mechanisms, even if the suspensions are assumed as rigid, the model roll motion is still one degree of freedom for the system.

Five state variables fully describe the state of the model state which are:

- longitudinal ( $u$ ) and lateral ( $v$ ) speed of the projection of the center of gravity on the road (point N);
- yaw velocity of the main frame ( $r$ );
- steering angle  $\delta$ ;
- roll angle  $\varphi$ .

Nine dynamic equilibrium equations were derived from the simplified model, along with four tire lateral constitutive equations (linear behaviour with respect to slip angle and camber) and eight congruence equations which relate the front and rear camber and slip angles and the inclination of the front and rear tilting mechanisms with the model state variables.

After suitable substitutions the system was linearized and written in the state space form and the eigenvalues and eigenvectors of the state matrix were computed for different longitudinal speed values in the range 0–40 m/s.

Figure 9 shows the real and imaginary parts of the most significant eigenvalues of the dynamic matrix.

The capsize mode [3, 4], which represent the vehicle fall aside, is non-oscillatory in the entire investigated range since its associate eigenvalues is always real and greater than zero, that means that the mode is unstable in the whole investigated speed range. The weave mode, which consists in a counter-phase oscillation of the steering wheel and the main frame, is characterized by two different real eigenvalues at very low longitudinal speed (non-oscillatory behavior) and two complex-conjugate eigenvalues (oscillatory behaviour) at higher longitudinal speed; the eigenvalue is stable since the real part of the eigenvalues is always negative and the oscillation frequency is in the range 0–1.5 Hz. The wobble eigenvalue, which consists in the oscillation (frequency 0–4.5 Hz) of the handlebar along the steering tube, in almost all the considered longitudinal speed range and becomes unstable at about 38 m/s: this value is way higher respect to the maximum allowed speed of the demonstrators. At very low speed, two different real eigenvalues were found which becomes two complex-conjugate eigenvalues at about 5 m/s. Finally, the rear wobble is a non-oscillatory and it is strongly stable in the whole considered longitudinal speed range and for this reason it is usually not deeply investigated in the literature [5].

The trend of the eigenvalues is similar to the ones already found for similar two and three wheelers [6]. The unstable eigenvalue related to the capsize exists, in different speed range, for every tilting vehicles and it is usually stabilized by the rider action.

## 4.2 Stability analysis of the tilting mechanism

Besides the analysis of the rigid vehicle eigenmodes, the suspension systems oscillations were considered separately. Indeed, once the right values of the spring and damping values of the front and rear shock absorbers were found considering classical ride dynamics [5, 7], additional possible oscillations arose, which do not exist in two-wheelers.

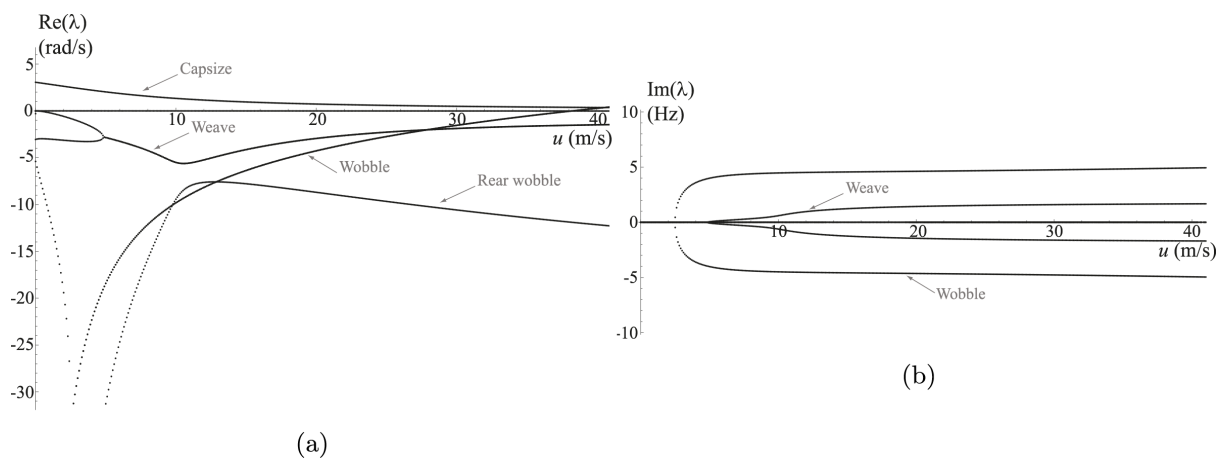


Figure 8. Real part (a) and imaginary part (b) of the eigenvalues of the rigid vehicle.

Figure 9a shows a simplified representation of the front tilting mechanism [8], which is composed by the front wheels, the inferior A-arms, the shock absorbers and the superior tilting lever which is linked to the main frame through a revolute joint. The mechanism is schematically summarized in Fig. 9b where a 3 degrees of freedom equivalent plane system is represented. The upper lever, which has inertia  $J_y$  computed about the rotation axis, can rotate by the angle  $\theta$  and the translation of the wheel masses  $m$  (which also includes the equivalent mass of the inferior A-arms) are related to the state variables  $y_1$  and  $y_2$ . The shock absorbers stiffness and damping,  $k$  and  $c$  respectively, are assumed constant and are obtained through the vehicle ride analysis (omitted).

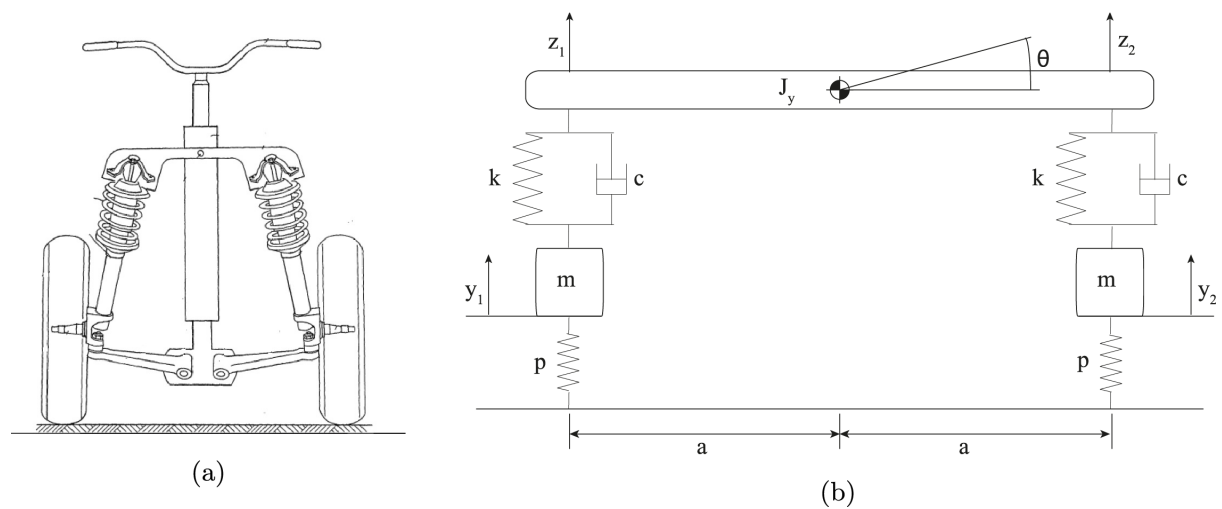


Figure 9. Tilting mechanism scheme (a) and model (b).

The dynamic equations were linearized considering the tilting mechanism in the central position and the eigenvalues and eigenvector were computed. The results, in terms of natural frequency and damping of each eigenmode, are shown in Fig. 10, as a function of the inertia of the tilting lever  $J_y$ .

Three natural modes can be identified which are ascribable to:

- Mode 1 rotation of the tilting lever and wheel masses fixed (red line);
- Mode 2 in-phase bounce of the wheel masses and tilting lever fixed (blue line);
- Mode 3 out of phase bounce of the wheel masses and rotation of the tilting lever (green line).

Mode 2 is, obviously, independent from the tilting lever inertia, since the body does not move. On the other hand, the tilting lever inertia influences the remaining two natural modes. In particular, if the inertia is low, the Mode 1 is over damped but the Mode 3 is almost not damped. This is due to the fact that, with low tilting lever inertia, the wheel masses have anti-symmetric displacement and the shock

absorber are not compressed since the tilting lever rotates in-phase with the wheels displacement. On the contrary, if the inertia is increased, the Mode 1 becomes oscillatory, even if it is strongly damped, and the Mode 1 is fairly damped: in this case, the rotation of the tilting lever and the anti-symmetric displacement of the wheel masses are not in phase and the damping element of the shock absorbers can actually dissipate energy.

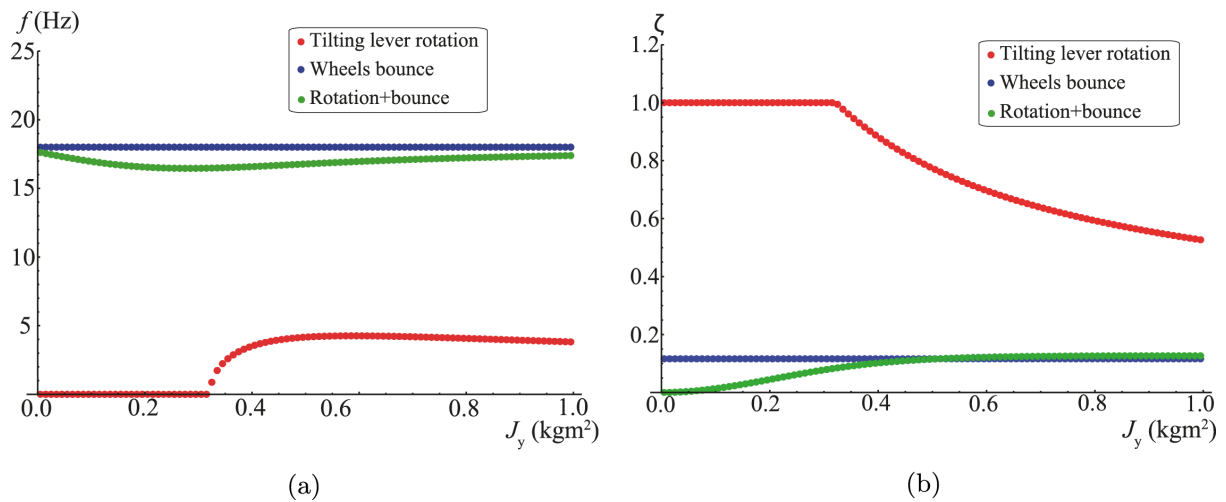


Figure 10. Natural modes of the tilting mechanism: frequency (a) and damping (b).

This analysis, even if performed with a simplified model, shows a possible issue of the tilting four-wheeler vehicles which does not exist in two wheelers and has to be taken into account to correctly design the tilting mechanism, in order to prevent undamped oscillations.

### 4.3 Multibody simulations

A multibody model of the vehicle was developed in MSC.Adams View environment. The model is made up of 32 rigid bodies connected through revolute, spherical and translational joints and it has 17 degrees of freedom, which can be ascribed to:

- three translations and three rotations of the whole vehicle assumed as a unique rigid body;
- four rotations of the wheels along their axis;
- four independent translations of the suspensions;
- two rotations of the tilting mechanism;
- one rotation of the handlebar along the steering tube.

The rider is assumed as a rigid body fixed to the main frame, the shock absorbers are modelled as constant stiffness and constant damping elements and the tire have radial compliance and non-linear longitudinal and lateral characteristics based on Pacejka model.

A virtual rider was implemented to reproduce the actual rider behaviour and was based on two independent controller [9]: the speed follower for the longitudinal dynamics and the roll follower for the lateral dynamics. In particular, the speed follower law, for each wheel, was determined on the basis of the following equations

$$T_{21} = \int_0^{\bar{t}} c_1(u_t(t) - u(t)) dt + c_2(u_t(t) - u(t)) + k(t) \quad (1)$$

$$T_{22} = \int_0^{\bar{t}} c_1(u_t(t) - u(t)) dt + c_2(u_t(t) - u(t)) - k(t) \quad (2)$$

where  $T_{21}$  and  $T_{22}$  are the rear left and rear right wheel traction torque respectively,  $c_1$  and  $c_2$  are controller parameters,  $u_t(t)$  is the target speed profile and  $u(t)$  is the actual longitudinal speed of the vehicle. The additional term  $k(t)$  can be added to a wheel and subtracted from the other without affecting the longitudinal dynamics of the vehicle. This term can be a very important peculiarity of four-wheelers and can be actively controlled in order to obtain desired yaw control, as in cars, or to prevent vehicle fall. Indeed, as it is discussed below, due to tilting mechanisms equilibrium, the longitudinal forces affects also the vertical loads on the wheels.

Concerning the roll follower, the handlebar velocity  $\dot{\delta}$  was determined as follows

$$\dot{\delta} = k_1 \ddot{\phi} + k_2 \dot{\phi} + k_3(\phi_t(t) - \phi(t)) \quad (3)$$

where  $k_1$ ,  $k_2$  and  $k_3$  are controller parameters,  $\phi_t(t)$  is the target roll angle profile and  $\phi(t)$  is the roll angle of the main frame.

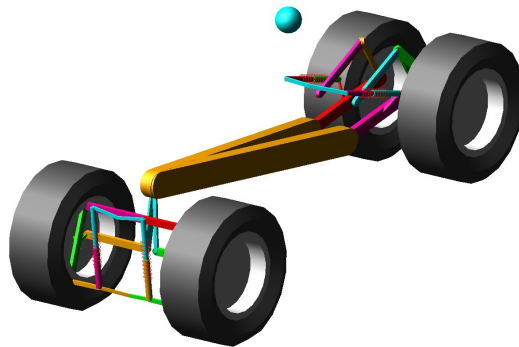


Figure 11. Multibody model in MSC.Adams View environment.

Figure 12 shows the results related to a manoeuvre composed by the vehicle acceleration from 0 to 30 km/h followed by a slalom. The vehicle accelerates up to the target speed in about 7 s (the acceleration time can be changed acting on the constants  $c_1$  and  $c_2$ ) and then keeps constant speed. Starting from  $t=10$  s the slalom manoeuvre begins: the actual roll follows the target roll profile with a delay of about 0.1 s and the steering wheel angle, which is computed integrating the law given in Eq. 3, is almost in counter-phase. This is a very important result: indeed, as already discussed in [9], the roll (and trajectory) of a tilting vehicle is not related, by an almost in-phase constant, to the steering input as it happens in cars.

Finally, Fig. 13–15 shows the results obtained in a constant speed (45 km/h) rightward steering pad manoeuvre where the target roll angle was assumed  $30^\circ$  and different constant values of  $k(t)$  (see Eq. 1–2) were imposed (i.e. zero, positive and negative). In particular, Fig. 13 shows the vertical loads on each tire, the target and actual roll angle and the steering angle during steering pad manoeuvre. Since the tire load are not statically determined, a load transfer is measured mainly on rear wheel, where the vertical load on the external wheel is higher than the one on the internal wheel. On the other hand, almost no load transfer is measured at front wheels. The steering wheel angle is initially leftward (counter-steering) and then rightward, as it happens in all tilting vehicle. This is a promising results since the driver probably will not perceive differences from classic tilting two-wheelers during normal ride.

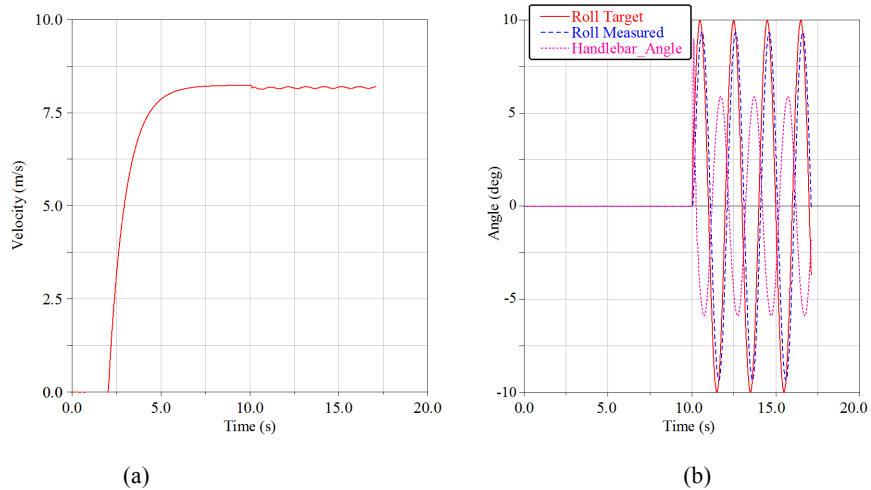


Figure 12. Vehicle speed (a) and vehicle roll (target and measured) along with steering angle (b) during acceleration and slalom manoeuvre.

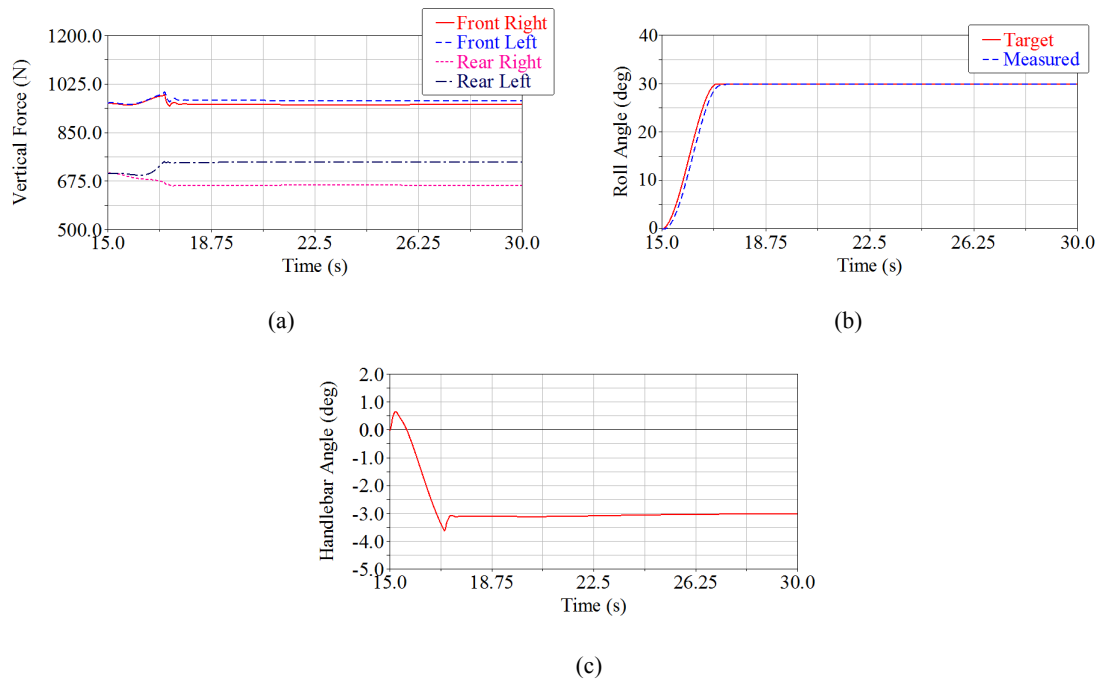


Figure 13. Vertical loads on wheels (a), target and actual roll angle (b) and handlebar angle (c) during steering pad manoeuvre –  $k(t)=0$ .

Fig. 14 shows the same manoeuvre performed with a constant positive  $k(t)$  value superimposed to the longitudinal dynamics controller (Eq. 1–2). The effect of  $k(t)$  does not affect neither the longitudinal speed (not represented) nor the roll angle but influences both the load transfer and the steering wheel angle. In particular, in this case the load transfer is increased with respect to the previous manoeuvres and the absolute value of the steering wheel angle necessary to keep the roll angle constant is reduced, resulting in a yawing effect on the vehicle lateral dynamics.



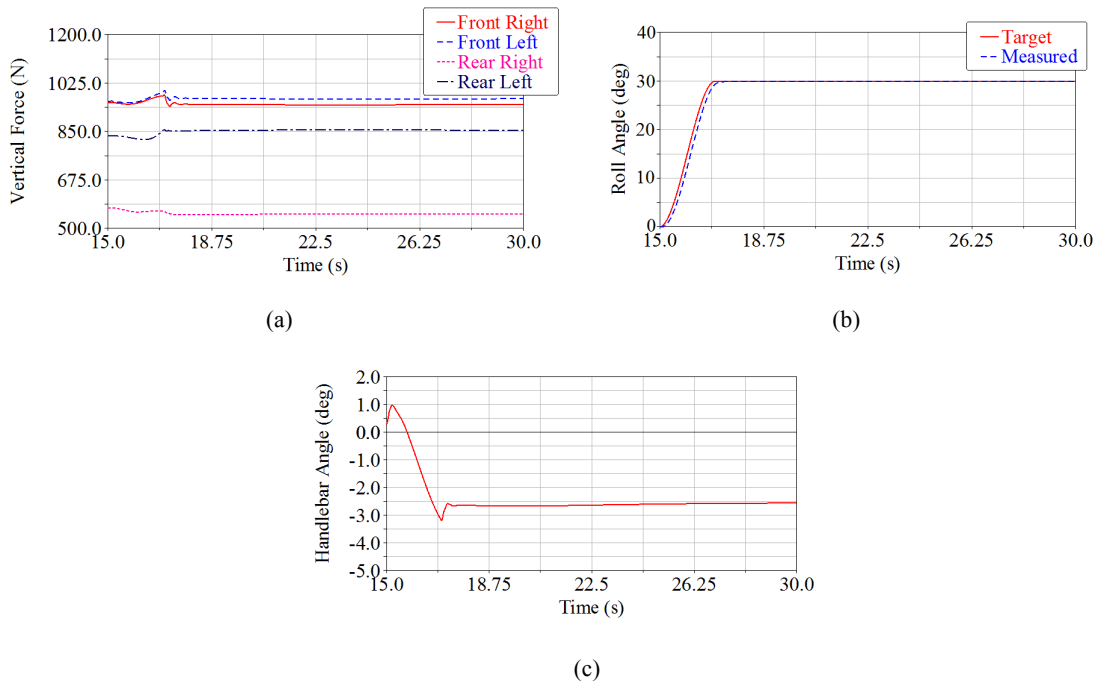


Figure 14. Vertical loads on wheels (a), target and actual roll angle (b) and handlebar angle (c) during steering pad manoeuvre –  $k = \text{const.} > 0$ .

On the contrary, if  $k(t)$  is assumed constant and negative (Fig. 15), the load transfer on rear wheels is inverted (load higher on the external wheel) and the steering wheel angle necessary to keep the roll angle constant is (in absolute value) greater, resulting in a counter yawing effect on the vehicle lateral dynamics.

These preliminary simulations showed the capability of the model and of the virtual rider to correctly reproduce different speed and roll angle profiles and highlighted some important peculiarities of tilting four wheelers. In particular, a strong bond between the longitudinal forces on the rear wheels (which can be controlled by the electronic differential) and the vehicle dynamics, both in terms of vertical loads at each wheel and rider inputs, arose which opens up the possibility of controlling the yaw dynamics in an active way. This can be strongly beneficial in aiding the rider in order to prevent otherwise uncontrollable fall events.

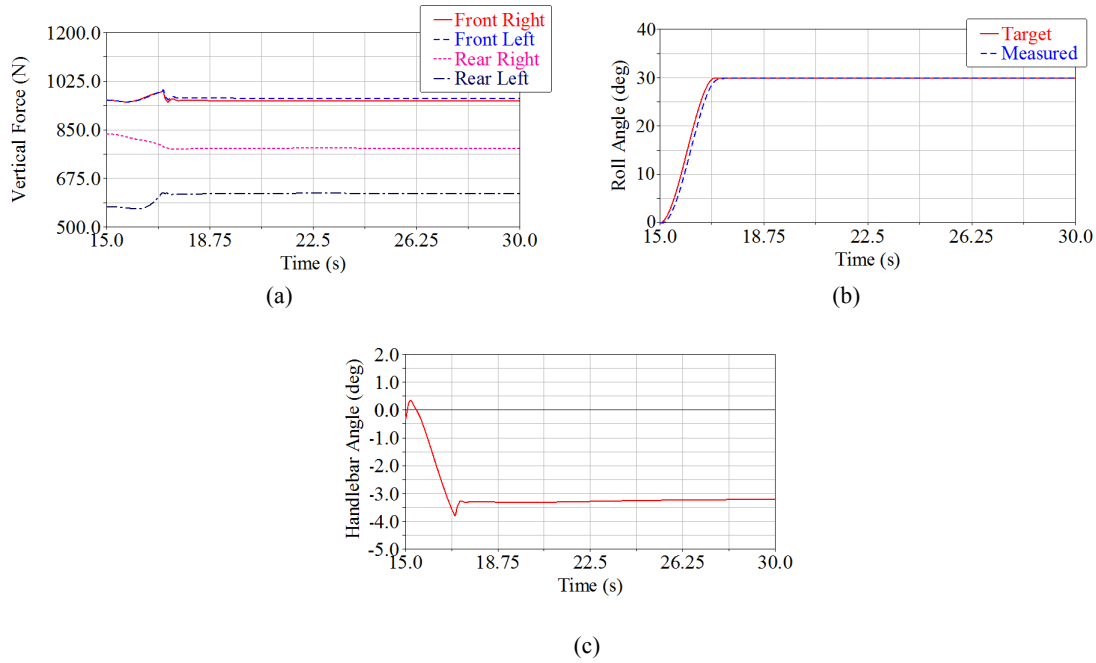


Figure 15. Vertical loads on wheels (a), target and actual roll angle (b) and handlebar angle (c) during steering pad manoeuvre –  $k = \text{const.} < 0$ .

## 5 Conclusions

L-category vehicles have the potential to be one of the key technologies for future urban mobility. The RESOLVE GV5 project is aimed to overcome the main limitations of the conventional three-four wheeler L-category products in terms of costs, energy efficiency and driving performance by the implementation of innovative vehicle concepts. Highly modular architectures, together with efficient batteries and electric drivetrain components as well as appropriate vehicle control systems will be used in order to develop lightweight and cost effective demonstrators. The tilting dynamic of the vehicles will be the key feature able to improve the handling performances and therefore the joy of use of these kinds of vehicles while maintaining limited lateral dimensions.

This paper focuses on the first steps of the virtual development of two vehicles in the L2 and L6 category. Using longitudinal simulation techniques and different driving cycles, the key performance of the vehicles was evaluated and the architecture of drivetrain and transmission was optimized guaranteeing the best compromise between energy efficiency and acceleration performances.

In a next step dedicated simulation models were developed to investigate the rigid vehicle stability, the stability of the tilting mechanism and handling behavior. The stability analysis results of the rigid vehicle showed a similar behavior compared to existing two and three wheelers on the market with a dominant unstable eigenvalue related to the capsizes that is typical for all tilting vehicles and stabilized by the rider steering actions.

A specific modal analysis of the tilting mechanism with suspension elements revealed three modes: (1) rotation of the tilting lever and wheel masses, (2) in-phase bounce of the wheel masses and tilting lever and (3) out of phase bounce of the wheel masses and rotation of the tilting lever. These modes are heavily influenced by the tilting architecture itself and a specific design approach must be followed in order to prevent undamped oscillations while maintaining limited masses and dimensions for the vehicles.

In the multibody simulations, a virtual rider was implemented in order to reproduce the actual rider behavior for investigating the vehicle kinematics and dynamics. As expected, no significant lateral load transfer was found while cornering on the two front wheels, but the strong influence of the traction forces on the rear vertical loads allows for promising future developments in terms of control strategies for an active differential system.

The simulation results obtained in this phase of the project will guide the definition of the final vehicle architectures for the two demonstrators: parts and components will be engineered and integrated in the vehicle concepts. A final phase of experimental testing will be performed on the two full scale prototypes and the results will be used in order to validate and, eventually, finely tune the simulation driven engineering approach.

## References

- [1] D Simic, H Lacher, C Kral, and F Pirker. Evaluation of the smartcooling (SC) library for the simulation of the thermal management of an internal combustion engine. Technical report, SAE Technical Paper, 2007.
- [2] D Simic. Simulation and evaluation of a powertrain of a hybrid electric all terrain vehicle (ATV). Technical report, International Advanced Mobility Forum, Geneva, Switzerland, 2010.
- [3] R S Sharp. The stability and control of motorcycles. *Journal of mechanical engineering science*, 13(5):316–329, 1971.
- [4] V Cossalter, R Lot, and F Maggio. The modal analysis of a motorcycle in straight running and on a curve. *Meccanica*, 39(1):1–16, 2004.
- [5] V Cossalter. *Motorcycle dynamics*. Lulu. com, 2006.
- [6] A Sponziello, F Frenzo, and M Guiggiani. Stability analysis of a three-wheeled motorcycle. *SAE International Journal of Engines*, 1(1):1396–1401, 2009.
- [7] M Guiggiani. *The Science of Vehicle Dynamics: Handling, Braking, and Ride of Road and Race Cars*. Springer Science & Business Media, 2014.
- [8] M Marcacci. Four-wheeler vehicle. *Patent EP*, 1694555B1, 2006.
- [9] F Bartaloni, O Di Tanna, F Frenzo, M Guiggiani, M Parenti, and A Sponziello. Dynamic analysis of a novel three wheeled tilting vehicle. In *poster presentation at IAVSD 20th Symposium, Berkeley CA*, 2007.